bioRxiv preprint doi: https://doi.org/10.1101/148825; this version posted June 11, 2017. The copyright holder for this preprint (which was not certified by peer review) is the author/funder, who has granted bioRxiv a license to display the preprint in perpetuity. It is made available under aCC-BY-NC-ND 4.0 International license.

Epistasis mediated alleviation of the cost of antibiotic resistance for MRSA.

Maho Yokoyama[1], Maisem Laabei[1], Emily Stevens[1], Sion Bayliss[1], Nicola Ooi[2], Alex O'Neill[2], Ewan Murray[3], Paul Williams[3], Anneke Lubben[4], Shaun Reeksting[4], Guillaume Meric[1], Ben Pascoe[1], Samuel K. Sheppard[1], Mario Recker[5], Laurence D. Hurst[1], and Ruth C. Massey[1,6]*

1: Milner Centre for Evolution, Dept. of Biology and Biochemistry, University of Bath, UK.
2: Antimicrobial Research Centre, Faculty of Biological Sciences, University of Leeds, Leeds, LS2 9JT, UK.
3: Centre for Biomolecular Sciences, University of Nottingham, NG7 2RD, UK.
4: Chemical Characterisation and Analysis Facility, Faculty of Science, University of Bath, BA2 7AY.
5: College of Engineering, Mathematics and Physical Sciences, University of Exeter, EX4 4QF, UK.
6: School of Cellular and Molecular Medicine, University of Bristol, UK.

* for correspondence: ruth.massey@bristol.ac.uk

bioRxiv preprint doi: https://doi.org/10.1101/148825; this version posted June 11, 2017. The copyright holder for this preprint (which was not certified by peer review) is the author/funder, who has granted bioRxiv a license to display the preprint in perpetuity. It is made available under aCC-BY-NC-ND 4.0 International license.

ABSTRACT

Understanding how multi-drug resistant pathogens evolve is key to identifying means of curtailing their further emergence. Theoretically, antibiotic resistance incurs a fitness cost to bacteria, however, the scale of this have been found to vary widely, with some resistance mechanisms reported to have little or no cost. One such apparently cost-free resistance mechanism acquired by the major human pathogen *Staphylococcus aureus* is to the clinically important antibiotic mupirocin, which is mediated by mutation of the isoleucyl-tRNA synthethase gene. In a recent GWAS study we reported that this mutation is associated with changes in the virulence of the bacteria, with the data suggesting this is driven through epistatic interactions with other loci. Here we report that in a subsequent geographically distinct collection of MRSA of the USA300 lineage we have found the same epistatic signal. We demonstrate that this resistance mutation reduces the expression of *S. aureus* toxins, which alleviates the costs associated with mupirocin resistance and explains the apparent lack of effect on fitness reported previously. Given the potential effect the mutation could have on enzyme activity and the subsequent translation of proteins containing high levels of isoleucine, we quantified the prevalence of isoleucine across all coding regions of the *S. aureus* genome. This identified key proteins of the toxin regulating Agr quorum sensing system, as well as four of the PSM family of toxins as having above average isoleucine content. For one of these proteins, AgrC, we found that shortly after induction there is a two-fold difference in the ability of the mupirocin resistant strain to translate the protein. We also found there to be significantly more free isoleucine in the cytoplasm of the mutant, suggesting it is not being incorporated into proteins at the same rate as the wild type strain. Although the effect of the mutation on AgrC translation was only temporary, we believe this delay in activation may have an effect on toxin expression, which in combination with the reduction in the expression of the PSMs may explain the effect on toxicity in the mupirocin resistant strain. This concomitant compensation of antibiotic resistance by offsetting the energetically-costly production of toxins through epistasis may help explain the rapid and successful emergence of this problematic antibiotic resistant pathogen.

bioRxiv preprint doi: https://doi.org/10.1101/148825; this version posted June 11, 2017. The copyright holder for this preprint (which was not certified by peer review) is the author/funder, who has granted bioRxiv a license to display the preprint in perpetuity. It is made available under aCC-BY-NC-ND 4.0 International license.

INTRODUCTION

Antibiotic resistance can evolve in many ways, and frequently incurs a fitness cost to the organism[1] which has to either mutate the target site of the antibiotic, acquire and express a gene encoding an alternative non-susceptible version of the target protein, or acquire an efflux pump that removes the antibiotic before it can attack its target[2]. As antibiotics are most commonly used for short and defined periods of time, bacteria are under selection to reduce these costs to avoid displacement once treatment has finished. In many cases this is achieved through compensatory mutations which has resulted in many resistance mechanisms being maintained stably in the population for long periods of time[3]. However, some antibiotic resistance mechanisms have been reported to incur no detectable fitness costs[4]. This could be due to limitations in our abilities to replicate *in vivo* situations sufficiently *in vitro*, but it could also suggest that bacteria can ameliorate fitness costs without mutation, which would be distinctly advantageous over those mechanisms that rely on the stochasticity of acquiring a specific compensatory mutation to maintain competitive fitness.

Staphylococcus aureus is an example of a major human pathogen[5] that has become more challenging to treat due to the emergence of antibiotic resistance, with Methicillin-Resistant *S. aureus* (MRSA) being the most notable example[6]. This bacterium resides asymptomatically as part of the normal nasal flora of up to 50% of humans[7], however, this is a significant risk factor for infection[8], to the extent that carriers are often decolonised using antibiotics such as mupirocin prior to invasive procedures such as surgery or dialysis[9]. Mupirocin is a polyketide antibiotic that is applied as an ointment to eradicate nasal carriage of MRSA in patients at risk of infection[10]. Such decolonisation has been reported to reduce *S. aureus* infections of post-surgical wounds by 58%, of haemodialysis patients by 80% and of peritoneal dialysis patients by 63%[11].

The molecular target for mupirocin is the bacterial isoleucyl-tRNA synthetase (IleRS), which charges tRNAs with the amino acid isoleucine (Ile)[10]. By binding to this enzyme the antibiotic halts protein synthesis, so inhibiting bacterial growth[12]. As a consequence of the widespread use of mupirocin, resistance has emerged where the bacteria have mutated the gene encoding IleRS, *ileS*, resulting in an amino acid

bioRxiv preprint doi: https://doi.org/10.1101/148825; this version posted June 11, 2017. The copyright holder for this preprint (which was not certified by peer review) is the author/funder, who has granted bioRxiv a license to display the preprint in perpetuity. It is made available under aCC-BY-NC-ND 4.0 International license.

substitution (V588F, encoded by a G to T single nucleotide polymorphism (SNP) at position 1,762 in the *ileS* gene) which alters the protein's structure and renders mupirocin less effective[13]. This confers a low to intermediate level of resistance to the antibiotic[14]. Alternatively, the bacteria acquire an alternative IleRS, encoded by a *mupA* or *mupB* gene, on a plasmid, which confers a higher level of resistance[15,16]. The prevalence of mupirocin resistance varies widely, with some reporting it to be as high as 80%[17], the clinical relevance of which is that decolonisation is less successful[18] resulting in increasing rates of infection in high risk patients.

The *ileS* gene is highly conserved across the thousands of sequenced *S. aureus* isolates, and many failed attempts to inactivate it suggest its activity is essential to the bacteria. It is therefore surprising that the mutation that confers mupirocin resistance, by altering the structure of the encoded protein does not appear to affect fitness. However, in a recent genome wide association study (GWAS) on the major hospital acquired MRSA clone, ST239, this mutation was significantly associated with differences in the virulence of *S. aureus* isolates[19]. Its effect on toxin secretion (a major aspect of *S. aureus* virulence) was believed to result from epistatic interactions between *ileS* and other polymorphic loci. That is, when the isolates were split into those with and without the mupirocin resistance conferring mutation in *ileS* (from here on referred to as mup^R IleRS), no significant difference in toxicity was detected. However, when the isolates were further stratified into those with and without the mup^R IleRS, alongside those with and without other polymorphic loci, significant differences in toxicity were observed with combinations of specific loci, suggesting that these loci interact with *ileS* in an epistatic manner to affect toxin production[19].

As isoleucine is a highly hydrophobic amino acid we would expect it to be prevalent in membrane embedded proteins. Such proteins play key roles in both the sensing of the environment to signal to the bacteria when to express toxin genes[20,21], but also in the destructive nature of the toxins that embed themselves in the membrane of host cells[22]. Toxin production is an energetically expensive activity which is often selected against during *S. aureus* infection, and as such we hypothesised that the emergence and success of the mupirocin resistance conferring mutation in the *ileS* gene is due in part to it reducing toxin expression through

bioRxiv preprint doi: https://doi.org/10.1101/148825; this version posted June 11, 2017. The copyright holder for this preprint (which was not certified by peer review) is the author/funder, who has granted bioRxiv a license to display the preprint in perpetuity. It is made available under aCC-BY-NC-ND 4.0 International license.

epistatic interactions with proteins containing high levels of isoleucine. Here we have characterised the fitness and toxicity affecting epistatic effects of the mup^{R} IleRS, and suggest our findings may explain the successful emergence of this notorious antibiotic resistant pathogen.

RESULTS and DISCUSSION

Epistasis between the mupirocin resistance conferring mutation in the *ileS* gene and other loci is associated with the toxicity of the USA300 MRSA lineage. In a previous study, which focussed on the hospital associated ST239 lineage of MRSA, we found that epistasis between the mupirocin resistance conferring mutation in the *ileS* gene and other loci was associated with the toxicity of individual isolates[19]. In a subsequent GWAS study on a genetically and geographically distinct collection of MRSA that contained 134 isolates of the USA300 lineage, we identified polymorphic loci directly affecting toxicity[23]. To examine whether there were any epistatic interactions affecting toxicity in the USA300 collection we used PLINK, an open source GWAS platform[24]. Here we again found the same mupirocin resistance conferring mutation in the *ileS* gene as identified within the ST239 collection as the most dominant epistatically interacting locus (fig. 1), demonstrating the widespread nature of this effect across a diverse set of clonal lineages.

The mupirocin resistance conferring mutation in the *ileS* gene affects bacterial toxicity. As our data is based on clinical isolates with many other polymorphic loci we aimed to functionally verify the effect of mupirocin resistance on toxicity. We isolated a mup^{R} verison of SH1000 by plating SH1000, a mup^{S} strain, on agar containing 4μg/ml mupirocin. The resulting mup^{R} colonies were subjected to whole genome sequencing to confirm the V588F mutation was present, and that no additional mutations in toxicity affecting loci had emerged; this strain was designated MY40. The toxicity of this mutant pair was quantified, where the wild type mupirocin sensitive parent strain killed 87% of the cells, whereas the mupirocin resistant mutant killed only 71% (two tailed t-test; p=0.023). This confirmed the negative effect of mupirocin resistance on the ability of *S. aureus* to lyse human cells.

bioRxiv preprint doi: https://doi.org/10.1101/148825; this version posted June 11, 2017. The copyright holder for this preprint (which was not certified by peer review) is the author/funder, who has granted bioRxiv a license to display the preprint in perpetuity. It is made available under aCC-BY-NC-ND 4.0 International license.

Reducing the production of toxins alleviates the fitness cost of mup^R. The *ileS* gene is both highly conserved and essential to the bacteria, as such it is surprising that mutations that alter the encoded proteins structure does not have an apparent effect on the fitness of the resistant bacteria. As the production and secretion of toxins is an energetically costly activity, we hypothesized that the down regulatory effect of mupirocin resistance on toxin production may mask or alleviate the resistance related fitness costs that are incurred. To test this we quantified the relative fitness[25] of mup^S and mup^R strains by competition in two genetic backgrounds; one in a wild type background where the bacteria can express toxins, and one where the major regulator of toxin expression, the Agr quorum sensing system, has been inactivated such that neither competing strain can produce toxins. As reported previously, in the wild type background with the functional Agr system, there was no difference in fitness between mup^S and mup^R strains, where the Malthusian parameters of the mup^S and mup^R strains were 14.9 and 14.8 respectively (two-tailed test p=0.6). However, when we quantified the relative fitness in the Agr defective background where neither strain could produce toxins, and so any alleviation of fitness that may result from the reduction of toxicity by the mup^R mutation was nullified, we found the fitness of the mup^R strain to be significantly lower than the mup^S strain, where the Malthusian parameters of the mup^S and mup^R strains were 15.0 and 14.4 respectively (two-tailed t-test; p=0.02). This demonstrates that this mutation can affect fitness, and that the alleviation of this burden by reducing toxin production which may explain the widespread success of this resistance mechanism.

Identification of proteins affecting toxicity via epistasis. To understand the mechanistic basis of how epistasis between mup^R IleRS and the other loci affects toxicity we compared the list of loci identified as interacting with mup^R IleRS for both the ST239 and USA300 collections (Table 1), however no known effectors of toxicity were identified amongst either collection. As GWAS is notorious for producing false positive associations, we hypothesised this may be hindering the use of this approach to identify plausible candidate loci that interact with ileS to affect toxicity. As such we focussed instead on the inherent activity of IleRS, which is to

bioRxiv preprint doi: https://doi.org/10.1101/148825; this version posted June 11, 2017. The copyright holder for this preprint (which was not certified by peer review) is the author/funder, who has granted bioRxiv a license to display the preprint in perpetuity. It is made available under aCC-BY-NC-ND 4.0 International license.

charge tRNA with isoleucine for incorporation into proteins, and argued that mutation of IleRS would have the greatest effect on proteins with the highest proportions of Ile. We therefore quantified the Ile content for each protein encoded across the *S. aureus* genome to which we fitted a regression model (after a Box-Cox power transformation) and then identified those proteins that fell outside the 95% prediction interval (fig. 3, Supp Table 1). Amongst these high Ile containing proteins are AgrB and AgrC at 18 and 17% respectively, the two membrane bound components of the Agr toxicity regulating, quorum sensing system. We also identified four known membrane damaging toxins: delta, PSMα1, PSMα2 and PSMα4 also contain exceptionally high levels of Ile (19.2% for delta, 28.6% for PSMα1 and PSMα2, and 40% for PSMα4). Based on these findings we hypothesised that were the translation of these proteins affected by the mutation of IleRS, this could explain how such epistatic interactions could be affecting toxicity.

The early translation of AgrC, a protein with high Ile content, is affected by mupirocin resistance. Despite being the primary focus of many research groups for decades, natively produced AgrB and AgrC proteins have never been visualised using existing detection methods, such as western blotting. As such, the quantification of the translation of these proteins is reliant on developing alternative assays as proxies for their abundance. The *agrC* gene encodes the membrane bound component of the Agr system that detects and responds to extracellular AIP and transmits this information through phospho relay to AgrA, which is the cytoplasmic response regulator of the Agr system. To determine the effect of mup^R IleRS on protein translation more directly, we engineered a *S. aureus* strain in which we could control the transcription of *agrC,* while simultaneously quantifying its translation (depicted in fig. 3). To achieve this, the *agr* locus in SH1000 was deleted and then partially replaced with a plasmid containing the *agrC* and *agrA* gene, where the *agrC* gene was engineered to encode a 6X his-tag at the C terminus to facilitate protein quantification using anti-his tag antibodies. This created MY42 (mup^S) and MY43 (mup^R), which have closed systems in which the rate of the response of the bacteria to the addition of exogenous AIP at both a transcriptional and translational level can be accurately controlled and monitored.

bioRxiv preprint doi: https://doi.org/10.1101/148825; this version posted June 11, 2017. The copyright holder for this preprint (which was not certified by peer review) is the author/funder, who has granted bioRxiv a license to display the preprint in perpetuity. It is made available under aCC-BY-NC-ND 4.0 International license.

Overnight cultures of MY42 and MY43 were diluted into fresh media and after 2h of growth 100nM of synthetic AIP-1 was added. After an hour of incubation the mRNA and whole cell proteins were extracted. Using qRT-PCR on the mRNA samples we detected no difference in the transcription of the *agrC* gene between the mup^R and mup^S strains, which was unsurprising given that they were induced with the same quantities of AIP for the same period of time (Table 2). However, when we compared the translation of the AgrC protein there was on average twice as much protein in the extraction from the mup^S strain when compared to that from the mup^R strain (Table 2), where a representative western blot can be seen in figure 4. This suggests that in the mupirocin resistant strain, proteins containing high levels of Ile such as AgrC, are translated less efficiently, despite equivalent amount of mRNA being available for translation.

The cytoplasm of mupirocin resistant *S. aureus* contains more free Ile. As our data suggests that the mup^R IleRS may affect the efficiency of incorporation of Ile into proteins, we hypothesised that there may be a detectable difference in the quantity of free Ile present in the cytoplasm of mup^R and mup^S strains. To test this we lysed overnight cultures of the isogenic mup^R and mup^S strains SH1000 and MY40, and quantified the free Ile present in their cytoplasm by LC-MS/MS. On average the mupirocin resistant strains had 5.5μg/ml of Ile in their cytoplasm, whereas the mupirocin sensitive strains only had 5.2 μg/ml (one-tailed T-test; p=0.03), providing further support for our hypothesis that mupirocin resistance affects the activity of IleRS.

The effect of mupirocin resistance on Agr activity is temporal. An alternative means of quantifying Agr activity is to monitor the transcription of the regulatory RNA molecules, which is responsible for the major phenotypic changes associated with this system, RNAIII. By utilising a lux fusion to the RNAIII promoter P3, we were able to monitor both the response of the system to increasing quantities of AIP, and also monitor its activity over time. The sensitivity of this system is such that activation of the Agr system is only detectable from 2hr post induction onwards. Using this experimental system we found no difference in the Agr activity between the mup^S

bioRxiv preprint doi: https://doi.org/10.1101/148825; this version posted June 11, 2017. The copyright holder for this preprint (which was not certified by peer review) is the author/funder, who has granted bioRxiv a license to display the preprint in perpetuity. It is made available under aCC-BY-NC-ND 4.0 International license.

and mup^{R} strains (fig. 5), suggesting any early effects of the mupirocin resistance mutation on AgrC translation is short lived.

Protein A, alpha toxin and PSMs production are affected by mupirocin resistance.

As the effect of the mupirocin resistance mutation on Agr seems to be short lived, we wanted to quantify its effect on Agr regulated genes. We therefore compared the level of PSMs produced by the mup^{S} and mup^{R} strains, and demonstrate that the expression of these Agr regulated toxins was affected by mupirocin resistance (fig. 6), although as four of these proteins contain high levels of Ile, we cannot verify at this stage if the effect on their production is at the transcription or translation stage. We also compared the expression of alpha toxin and Protein A, and found that as would be expected were the Agr activity of the system repressed, that alpha toxin expression is lower (2.12 fold, $p=0.02$) while Protein A is higher (27 fold, $p<0.001$) in the mup^{R} strain, a representative western is provided in fig. 6.

Conclusion

The application of GWAS to understand bacterial phenotypes is growing in popularity, but it is notorious for producing false positive associations, which is further compounded by the effects of population structure and linkage disequilibrium. For this reason, it was not until we confirmed previously identified virulence-affecting, epistatic interactions in a second, genetically and geographically distinct collection of *S. aureus* that we began characterising its mechanistic basis. In doing so we have demonstrated that mupirocin resistance reduces the toxicity of *S. aureus,* an effect we believe it mediated through slowing of the translation of proteins containing high levels of isoleucine, such as those of the toxicity regulating Agr system. This reduction in toxin expression appears to alleviate the fitness costs associated with this antibiotic resistance mechanism, which may provide a explaining the successful emerges of this problematic pathogen, as toxin expression or are often switched off by mutation during infection[23].

bioRxiv preprint doi: https://doi.org/10.1101/148825; this version posted June 11, 2017. The copyright holder for this preprint (which was not certified by peer review) is the author/funder, who has granted bioRxiv a license to display the preprint in perpetuity. It is made available under aCC-BY-NC-ND 4.0 International license.

MATERIALS AND METHODS

Strains and growth conditions

All strains used in this study are listed in Table 2. *S. aureus* strains were grown at 37°C, in either tryptic soy agar or broth (TSA/TSB) with the appropriate antibiotic where necessary. The *E. coli* TOP10 strain containing the pAgrC(his)A plasmid was grown in Luria-Bertani (LB) media with 100µg/ml ampicillin. THP-1 cells were grown in RPMI 1640 supplemented with foetal bovine serum (10%), L-glutamine (2mM), penicillin (100 units/ml) and streptomycin (100µg/ml) and incubated at 37°C with 5% CO_2.

Selection of the mupirocin resistant strain.

As an essential gene *ileS* cannot be inactivated, and as a consequence a homologous recombination based mutational approach were unsuccessful. Therefore, to generate isogenic mupirocin resistant and sensitive strains we utilised a selection based method where an overnight culture of a mupirocin sensitive strain (e.g SH1000 (derivative of NCTC 8325, NCBI accession: NC_007795.1)) was plated onto agar plates with 4µg/ml mupirocin. This was incubated at 37°C for 48 hr and colonies that grew were further isolated by streaking onto fresh mupirocin plates.

Genome sequencing of the mup^R strain.

S. aureus strain MY40 was sequenced in this study; DNA was extracted using the QIAamp DNA Mini Kit (QIAGEN, Crawley, UK), using manufacturer's instructions with 1.5 µg/µL lysostaphin (Ambi Products LLC, NY, USA) to facilitate cell lysis. DNA was quantified using a Nanodrop spectrophotometer, as well as the Quant-iT DNA Assay Kit (Life Technologies, Paisley, UK) before sequencing. High-throughput genome sequencing was performed using a MiSeq machine (Illumina, San Diego, CA, USA) and the short read, paired-end data was assembled using the *de novo* assembly algorithm SPAdes (Bankevich et al (SPADES). Sequence data are archived in the NCBI repositories: GenBank Accession: SUB2754769, Short Read Archive (SRA): SRR5651527, associated with BioProject: PRJNA384009. Assembled genomes are also available on FigShare (doi.org/10.6084/m9.figshare.5089939.v1).

bioRxiv preprint doi: https://doi.org/10.1101/148825; this version posted June 11, 2017. The copyright holder for this preprint (which was not certified by peer review) is the author/funder, who has granted bioRxiv a license to display the preprint in perpetuity. It is made available under aCC-BY-NC-ND 4.0 International license.

Toxicity assays

THP-1 cells[26] were grown as described above and harvested by centrifugation and washed in PBS and diluted to a final density (determined by haemocytometer) of $2x10^6$ cells per ml of PBS. Bacterial supernatant was harvested after 18hrs of growth in TSB at 37°C. 20µl of the bacterial supernatant was mixed with 20µl of THP-1 cells, and incubated for 12 mins at 37°C. 260µl of Guava ViaCount (Milipore) was added to the sample, and incubated at room temperature for 5 mins before analysing the viability on the Guava flow cytometer (Milipore).

Competition assay.

Two pairs of strains, SH1000 and MY40 (mup^S and mup^R, both Agr positive), and MY18 and MY41 (mup^S and mup^R, both Agr negative), were co-cultured to see if there was a fitness cost associated with mup^R. The strains were cultured individually overnight and diluted to 10^4 cfu/ml. 25µl of each diluted culture was added into 5ml fresh broth, and grown at 37°C with shaking for 24h. The mixed culture was diluted and plated onto agar plates with and without 4µg/ml mupirocin and incubated at 37°C. The resulting colonies were counted, and the number of colonies from the mupirocin plate was subtracted from the count from no antibiotic plate. The Malthusian parameter was calculated using the following formula:

Ln (final density (colony forming units (CFU)/ml) / starting density (CFU/ml))

The Malthusian parameters of the mup^S and mup^R strains were compared using a t-test.

Deletion of the Agr locus from SH1000.

Phage transduction was used to construct the mup^R and mup^S Agr mutants. In the *S. aureus* strain ROJ48, the entire Agr locus has been replaced with an erythromycin resistance cassette and a P3-lux system[27]. This was moved from ROJ48 into SH1000 by phage transduction as follows: ROJ48 φ11 lysates were prepared from 200µl of overnight ROJ48 culture in LK (1% Tryptone, 0.5% yeast extract, 1.6% KCl) which was added to 3ml of fresh LK and 3ml of phage buffer (10mM $MgSO_4$, 4mM $CaCl_2$, 50mM Tris-HCl pH 7.8, 100mM NaCl and 0.1% gelatine powder in molecular/MiliQ water), and to this 500µl φ11-RN6390B lysate was added. This was incubated at 30°C

bioRxiv preprint doi: https://doi.org/10.1101/148825; this version posted June 11, 2017. The copyright holder for this preprint (which was not certified by peer review) is the author/funder, who has granted bioRxiv a license to display the preprint in perpetuity. It is made available under aCC-BY-NC-ND 4.0 International license.

shaking until the media became clear, which indicated bacterial lysis. The lysates were then filter sterilised, and a second round of lysis was carried out on ROJ48 with this first round lysate. After these two lysis steps, transduction into SH1000 strains was performed by adding 200µl of overnight culture to 1.8ml LK with 10µl 1M $CaCl_2$, and 500µl the φ11-ROJ48 lysate. This was incubated at 37°C with shaking for 45 min, then 1ml ice cold 20mM trisodium citrate was added and the transducing mixture was placed on ice for 5 min. The bacteria were harvested by centrifugation and re-suspended with 1ml ice cold 20mM trisodium citrate. This was incubated on ice for 2.5h, and plated onto TSA plates with 20mM trisodium citrate, erythromycin and lincomycin (25µg/ml) which was incubated overnight at 37°C.

AIP EC50 and AIP quantification assays

These assays were performed as described previously[27]. Strains were grown overnight in Brain Heart Infusion (BHI), and 1ml of the overnight was washed 3 times with PBS. The pellet was re-suspended in fresh BHI and grown for a further 2h. A dilution series of AIP-1 was created, with concentrations ranging from 250nM to 0.125nM in 1:2 dilutions, plus 1250nM and 2500nM. 190µl of the culture was pipetted into a black 96-well plate, and 10µl of this dilutions series were also pipetted into the wells. The OD_{600} and luminescence readings were carried out every 15 min.s for 80 cycles in a Tecan plate reader. For the AIP quantification strains were grown in BHI, with chloramphenicol (10µg/ml). The reporter strain was diluted 1/20 into fresh BHI and grown for a futher 2h, while the supernatants of the mupS and mupR strains (SH1000, MY40, MY18 and MY41) were filtered through a 0.22µm filter. The reporter strain was diluted 1/50 and pipetted into a black 96-well plate. The supernatant was added to the wells at 5% final concentration, and the OD_{600} and luminescence readings were carried out every 15 mins for 80 cycles in a Tecan plate reader.

Construction of pAgrC(his)A (with his-tag)

The His tagged agrC vector was constructed by Site-Directed Mutagenesis of the plasmid pAgrCA[27] based on the Stratagene Quick change methodology using primer pair EJM 84 (5' CAAAAAGTTGAAATTATTAACAAC **CACCATCACCATCATCAC**

bioRxiv preprint doi: https://doi.org/10.1101/148825; this version posted June 11, 2017. The copyright holder for this preprint (which was not certified by peer review) is the author/funder, who has granted bioRxiv a license to display the preprint in perpetuity. It is made available under aCC-BY-NC-ND 4.0 International license.

TAGCCATAAGGATGTGAATGTATG (His tag and new stop codon in **bold**)) and EJM85 (5' GTGGTTGTTAATAATTTCAACTTTTTGAATAAAGAAACC ATTTTCGATAATTG).

Transformation of pAgrC(his)A into the Agr knock out strains.

pAgrC(his)A was extracted from *E. coli* TOP10. First, this plasmid was electroporated into RN4220; briefly, RN4220 was grown overnight in Brain Heart Infusion (BHI) medium, and diluted 1:500 into 10ml fresh BHI. This was then incubated at 37^{o}C with shaking until OD_{600} 0.4-0.6. The culture was then cooled, before centrifuging at 5,000rpm for 10 min at 4^{o}C. The media was discarded, and the pellet was re-suspended with 5ml ice cold 500mM sucrose. This was then re-centrifuged, supernatant discarded then 5ml ice cold 500mM sucrose added to the pellet. This above process was repeated 2 more times for a total of 3 sucrose washes, and centrifuged as above. After discarding the supernatant, 500µl ice cold 500mM sucrose was added to the pellet and re-suspended. This was left on ice for 30 min, before centrifuging and re-suspending in 100µl ice cold 500mM sucrose. The cells were pipetted into an electroporation cuvette, and 5-10µl pAgrC(his)A was added. This was then electroporated using the StA setting on MicroPulser (Bio-Rad), and then recovered in 750µl BHI at 37^{o}C for 1h. 200µl of the transformed material was plated onto TSA plates with chloramphenicol, and incubated overnight at 37^{o}C. The plasmid was extracted from the transformed RN4220, and electroporated into the agr knock out strains to yield MY42 (mup^{S}) and MY43 (mup^{R}).

qRT-PCR

Overnight cultures of MY42 and MY43 were diluted 1:500 into 3ml fresh TSB-chloramphenicol. This was grown for 2h, and induced with 100nM AIP-1 for 1h. 2ml of these cultures were mixed with 4ml RNA Protect Bacteria (Qiagen), and the RNeasy Mini Kit (Qiagen) was used to extract RNA following the manufacturer's protocol. Lysostaphin (200µg/ml) was added to Tris-EDTA buffer (Ambion), and this was added to the sample after the RNA Protect step before continuing with the protocol. When the RNA was extracted, Turbo DNA-free kit (Thermo) was used to remove genomic DNA from the RNA samples; 3µl Turbo DNase was added to the sample and incubated for 1.5h at 37^{o}C, the a further 4µl Turbo DNase was added and

bioRxiv preprint doi: https://doi.org/10.1101/148825; this version posted June 11, 2017. The copyright holder for this preprint (which was not certified by peer review) is the author/funder, who has granted bioRxiv a license to display the preprint in perpetuity. It is made available under aCC-BY-NC-ND 4.0 International license.

incubated for 1.5h. 35µl DNase inactivation reagent was added to the samples to inactivate the DNase according to the protocol. The concentration of RNA in the samples were measured using Qubit RNA Broad Range kit (Thermo) and normalised before using QuantiTect Reverse Transcription Kit (Qiagen) to convert the RNA samples into cDNA according to the manufacturer's protocol. After adding the reverse transcriptase, the samples were incubated at 42^{o}C for 20 min before raising the temperature to 95^{o}C for 3 mins to inactivate the reverse transcriptase. Primers for *gyrB*, a housekeeping gene, was used alongside those for *agrC* to standardise transcript levels (gyrB forward: CCAGGTAAATTAGCCGATTGC, gyrB reverse: AAATCGCCTGCGTTCTAGAG. agrC forward: GCAGATTATTCTATACTGTGCTAAC, agrC reverse: ACTACAAAAAAGCTAGGGAATATTACAAA). ssoAdvanced SYBR Green Supermix (Bio-Rad) was used, using a standard curve of known genomic DNA concentrations for each primer set. 5µl of samples, standards and water were pipetted into the wells of a 96-well PCR plate. The supermix was added to water and primers according to the manufacturer's protocol, and 15µl of this mix was pipetted over the DNA samples. This was then placed into a qPCR machine, and run using the manufacturer's recommendation. The quantity of *agrC* or RNA III cDNA was divided by the quantity of *gyrB* cDNA to get a ratio of *agrC* transcription levels.

An overnight culture of SH1000 and MY40 was diluted 1:1000 into 50ml fresh TSB, and grown for 18h. The cultures were centrifuged at 18,000 rpm for 10 min.s, and 35ml of the supernatant was mixed with 10ml butanol. The samples were incubated at 37°C shaking for 3h, and were then centrifuged at 3,000 rpm for 3 min and 1ml of the upper organic layer was taken off. The samples were then freeze-dried overnight and then re-suspended in 160µl 8M urea.

Western blots. To quantify AgrC translation overnight cultures of MY42 and MY43 were diluted 1:500 into 30ml fresh TSB. This was grown for 2h, and induced with AIP for 1h as above. The cells were pelleted and washed three times with phosphate buffered saline (PBS) (Oxoid). The pellet was re-suspended in 100µl PBS and lysostapin (200µg/ml), DNase I (20µg/ml) and RNase A (10µg/ml) was added to the cells, and incubated at 37^{o}C for 1h. The samples were then sonicated briefly on ice,

bioRxiv preprint doi: https://doi.org/10.1101/148825; this version posted June 11, 2017. The copyright holder for this preprint (which was not certified by peer review) is the author/funder, who has granted bioRxiv a license to display the preprint in perpetuity. It is made available under aCC-BY-NC-ND 4.0 International license.

and the lysate was mixed with 100µl PBS with 0.2% Triton X-100. Western was carried out using HisProbe HPR Conjugate (Thermo). The total protein concentration of two samples from each time point were equalised using Bradford Reagent (Sigma). 8µl of these samples were mixed with 8µl Morris SDS-PAGE sample buffer. The samples were then incubated at 60^{o}C for 2 min, before loading 15µl into 12% acrylamide gels. 5µl pre-stained protein ladder was added to a free well, and the gel was run at 200V for 1h. The proteins from the gel were transferred onto nitrocellulose membrane by wet transfer (400mA for 1h) and blocked in 50ml 5% skimmed milk for 1h on a shaking platform or 4°C overnight. It was then washed 4 times with 15ml TBS-T (25mM Tris-HCl, 150mM NaCl (pH7.2), 0.05% Tween 20) on a shaking platform for 10 min each. The membrane was then incubated with HisProbe working solution (1 part TBS (10mM Tris-HCl and 150mM NaCl (pH7.4)), 3 parts above TBS-T, 1:2000 HisProbe (4mg/ml), 1% Bovine Serum Albumin (Sigma)) for 1h on a shaking platform. The above wash process was then used twice, and the membrane was then placed onto SuperSignal West Pico Chemiluminescent Substrate (Thermo) working solution for 5 min before visualising. Densitometry using ImageJ was carried out to quantify the intensity of the bands.

To visualise α-toxin and protein A, a Western blot was carried out as follows: SH1000 (mupS) and MY40 (mupR) were grown for 18h in 15ml TSB, and the cells were pelleted by centrifugation at full speed for 10 min.s. Trichloroacetic acid was added to the supernatant to a final concentration of 20%, and the samples were incubated on ice for 1h. The samples were then centrifuged at full speed for 20 min.s at 4°C, and the supernatant discarded. 300µl cold acetone was added to the samples to dissolve the pellet, and then centrifuged again for 20 min.s at 4°C. This acetone step was repeated two more times, and then the pellet was re-suspended in 80µl 8M Urea and 0.5µl 1M NaOH. The samples were quantified, equalised, then mixed with Morris SDS-PAGE buffer as above, and incubated at 95°C for 5 min.s. before loading onto a 12% acrylamide gels as above. The gels were run at 120V for 1.5h, and the proteins were transferred onto nitrocellulose as above.

bioRxiv preprint doi: https://doi.org/10.1101/148825; this version posted June 11, 2017. The copyright holder for this preprint (which was not certified by peer review) is the author/funder, who has granted bioRxiv a license to display the preprint in perpetuity. It is made available under aCC-BY-NC-ND 4.0 International license.

For the α-toxin Western; the membrane was blocked in 5% skimmed milk at 4°C overnight and then washed 5x with PBS. It was incubated with rabbit anti α-toxin antiserum (1:3000 in PBS) for for 2h on a shaking platform, and washed 5x in PBS. Protein G-HRP Conjugate (1:1000 PBS) (Invitrogen) was added to the membrane, and incubated on a shaking platform for 1h. This was then visualised using the Opti-4CN Substrate Kit (BioRad) according to the manufacturer's guidelines.

For the protein A Western; the membrane was blocked in 5% skimmed milk for 1h on a shaking platform, and washed 5x with PBS. This was then incubated with the anti-protein A-HRP Conjugate (1:5000 in PBS) (Abcam) for 1h. The membrane was washed 5 times with PBS and visualised using the SuperSignal West Pico Chemiluminescent Substrate as before.

Cytoplasmic preps and LC-MS/MS quantification of isoleucine

5ml cultures of SH1000 and MY40 were grow for 18h. The cultures were then washed 3 times with 1ml sterile saline, centrifuging at 14,000rpm for 10 min after each wash. The pellet was then re-suspended in 500µl sterile saline, and 200µg/ml lysostaphin, 10µg/ml RNase A and 20µg/ml DNase I was added. This was then incubated at 37^{o}C for 1h, and sonicated briefly on ice. The samples were then centrifuged at 14,000rpm for 10 min, and 500µl of the resulting supernatant was applied to a Vivaspin 500 (3,000 NWCO) protein concentrator (GE Healthcare). This was then centrifuged at 15,000g for 30 min. The samples were analysed using Liquid Chromatography-mass spectrometry (LC-MS), similar to the protocol by Sowell et al[28]. This was carried out using a MaXis HD quadrupole electrospray time-of-flight (ESI-QTOF) mass spectrometer (Bruker Daltonik GmbH, Bremen, Germany) operated in ESI positive-ion MS mode. The QTOF MS was coupled to an Ultimate 3000 UHPLC (Thermo Fisher Scientific, California, USA). The capillary voltage was set to 4500 V, nebulizing gas at 2 bar, drying gas at 10 L/min and 200°C. The TOF scan range was from 50 – 600 mass-to-charge ratio (m/z). Liquid chromatography separation was performed using an Acquity UPLC BEH C18, 1.7 µM, 2.1 x 50 mm reverse phase column (Waters, Milford, MA, USA) with a flow rate of 0.3 mL/min at 30°C and an injection volume of 1 µL. Mobile phases A and B consisted of 0.1 % v/v formic acid in

bioRxiv preprint doi: https://doi.org/10.1101/148825; this version posted June 11, 2017. The copyright holder for this preprint (which was not certified by peer review) is the author/funder, who has granted bioRxiv a license to display the preprint in perpetuity. It is made available under aCC-BY-NC-ND 4.0 International license.

water, and 0.1 % v/v formic acid in acetonitrile, respectively. Gradient elution was carried out with 1 % mobile phase B until 2 min followed by a linear gradient to 95 % B at 4 min, holding at 95 % B until 6.5 min, and returning to 1 %B at 7 mins, with a total run time of 10 mins. The MS instrument was calibrated using a range of sodium formate clusters introduced by 10 µL loop-injection prior to the chromatographic run. The mass calibrant solution consisted of 3 parts of 1 M NaOH to 97 parts of 50:50 water:isopropanol with 0.2% formic acid. The observed mass and isotope pattern perfectly matched the corresponding theoretical values as calculated from the expected elemental formula. Isoleucine was detected as $[M + H]^+$ and $[M + Na]^+$ ions with a mass-to-charge (*m/z*) ratio of 132.1019 and 154.0838 within 0.005 Da, respectively. Data processing was performed using the Data Analysis software version 4.3 (Bruker Daltonik GmbH, Bremen, Germany). Five DL-isoleucine standards were at different concentrations were made up in in 0.1% formic acid, and analysed before and after the samples for quantification purposes.

bioRxiv preprint doi: https://doi.org/10.1101/148825; this version posted June 11, 2017. The copyright holder for this preprint (which was not certified by peer review) is the author/funder, who has granted bioRxiv a license to display the preprint in perpetuity. It is made available under aCC-BY-NC-ND 4.0 International license.

REFERENCES

1. Moura de Sousa, J., Balbontín, R., Durão, P. & Gordo, I. Multidrug-resistant bacteria compensate for the epistasis between resistances. *PLOS Biol.* **15,** e2001741 (2017).
2. Tenover, F. C. Mechanisms of Antimicrobial Resistance in Bacteria. *Am. J. Med.* **119,** S3–S10 (2006).
3. Levin, B. R., Perrot, V. & Walker, N. Compensatory mutations, antibiotic resistance and the population genetics of adaptive evolution in bacteria. *Genetics* **154,** 985–997 (2000).
4. Hurdle, J. G. The isoleucyl-tRNA synthetase mutation V588F conferring mupirocin resistance in glycopeptide-intermediate Staphylococcus aureus is not associated with a significant fitness burden. *J. Antimicrob. Chemother.* **53,** 102–104 (2003).
5. Rasigade, J.-P. & Vandenesch, F. Staphylococcus aureus: a pathogen with still unresolved issues. *Infect. Genet. Evol.* **21,** 510–4 (2014).
6. Lowy, F. Antimicrobial resistance: the example of *Staphylococcus aureus*. *J. Clin. Invest.* **111,** 1265–1273 (2003).
7. Wertheim, H. F. *et al.* The role of nasal carriage in Staphylococcus aureus infections. *Lancet Infect. Dis.* **5,** 751–762 (2005).
8. Gordon, R. J. & Lowy, F. D. Pathogenesis of Methicillin-Resistant *Staphylococcus aureus* Infection. *Clin. Infect. Dis.* **46,** S350–S359 (2008).
9. Abad, C. L., Pulia, M. S. & Safdar, N. Does the Nose Know? An Update on MRSA Decolonization Strategies. *Curr. Infect. Dis. Rep.* **15,** 455–464 (2013).
10. Thomas, C. M., Hothersall, J., Willis, C. L. & Simpson, T. J. Resistance to and synthesis of the antibiotic mupirocin. *Nat. Rev. Microbiol.* **8,** 281–289 (2010).
11. Simor, A. E. Staphylococcal decolonisation: An effective strategy for prevention of infection? *Lancet Infect. Dis.* **11,** 952–962 (2011).
12. Bertino Jr, J. S. Intranasal mupirocin for outbreaks of methicillin- resistant Staphylococcus aureus. *Am J Heal. Pharm* **54,** 2185–2191 (1997).
13. Antonio, M., McFerran, N. & Pallen, M. J. Mutations affecting the Rossman fold of isoleucyl-tRNA synthetase are correlated with low-level mupirocin resistance in Staphylococcus aureus. *Antimicrob. Agents Chemother.* **46,** 438–442 (2002).
14. Patel, J. B., Gorwitz, R. J. & Jernigan, J. A. Mupirocin Resistance. *Clin. Infect. Dis.* **49,** 935–941 (2009).
15. Udo, E. E. & Sarkhoo, E. Genetic analysis of high-level mupirocin resistance in the ST80 clone of community-associated meticillin-resistant Staphylococcus aureus. *J. Med. Microbiol.* **59,** 193–199 (2010).
16. Seah, C. *et al.* MupB, a New High-Level Mupirocin Resistance Mechanism in Staphylococcus aureus. *Antimicrob. Agents Chemother.* **56,** 1916–1920 (2012).
17. Hetem, D. J. & Bonten, M. J. M. Clinical relevance of mupirocin resistance in Staphylococcus aureus. *J. Hosp. Infect.* **85,** 249–256 (2013).
18. Hurdle, J. G., O'Neil, A. J., Mody, L., Chopra, I. & Bradley, S. F. In vivo transfer of high-level mupirocin resistance from Staphylococcus epidermidis to methicillin-resistant Staphylococcus aureus associated with failure of mupirocin prophylaxis. *J Antimicrob Chemother* **56,** 1166–1168 (2005).
19. Laabei, M. *et al.* Predicting the virulence of MRSA from its genome sequence.

bioRxiv preprint doi: https://doi.org/10.1101/148825; this version posted June 11, 2017. The copyright holder for this preprint (which was not certified by peer review) is the author/funder, who has granted bioRxiv a license to display the preprint in perpetuity. It is made available under aCC-BY-NC-ND 4.0 International license.

Genome Res. **24,** 839–849 (2014).

20. Novick, R. P. *et al.* Synthesis of staphylococcal virulence factors is controlled by a regulatory RNA molecule. **12,** 3967–3975 (1993).
21. Lina, G. *et al.* Transmembrane topology and histidine protein kinase activity of AgrC, the agr signal receptor in Staphylococcus aureus. *Mol. Microbiol.* **28,** 655–662 (1998).
22. Dinges, M. M., Orwin, P. M. & Schlievert, P. M. Exotoxins of Staphylococcus aureus. *Clin. Microbiol. Rev.* **13,** 16–34 (2000).
23. Laabei, M. *et al.* Evolutionary Trade-Offs Underlie the Multi-faceted Virulence of Staphylococcus aureus. *PLoS Biol.* **13,** 1–21 (2015).
24. Purcell, S. *et al.* PLINK: A Tool Set for Whole-Genome Association and Population-Based Linkage Analyses. *Am. J. Hum. Genet.* **81,** 559–575 (2007).
25. Lenski, R. E., Rose, M. R., Simpson, S. C. & Tadler, S. C. Long-Term Experimental Evolution in Escherichia coli. I. Adaptation and Divergence During 2,000 Generations. *Am. Nat.* **138,** 1315–1341 (1991).
26. Tsuchiya, S. *et al.* Establishment and characterization of a human acute monocytic leukemia cell line (THP-1). *Int. J. Cancer* **26,** 171–176 (1980).
27. Jensen, R. O., Winzer, K., Clarke, S. R., Chan, W. C. & Williams, P. Differential Recognition of Staphylococcus aureus Quorum-Sensing Signals Depends on Both Extracellular Loops 1 and 2 of the Transmembrane Sensor AgrC. *J. Mol. Biol.* **381,** 300–309 (2008).
28. Sowell, J., Pollard, L. & Wood, T. Quantification of branched-chain amino acids in blood spots and plasma by liquid chromatography tandem mass spectrometry for the diagnosis of maple syrup urine disease. *J. Sep. Sci.* **34,** 631–639 (2011).

bioRxiv preprint doi: https://doi.org/10.1101/148825; this version posted June 11, 2017. The copyright holder for this preprint (which was not certified by peer review) is the author/funder, who has granted bioRxiv a license to display the preprint in perpetuity. It is made available under aCC-BY-NC-ND 4.0 International license.

FIGURES

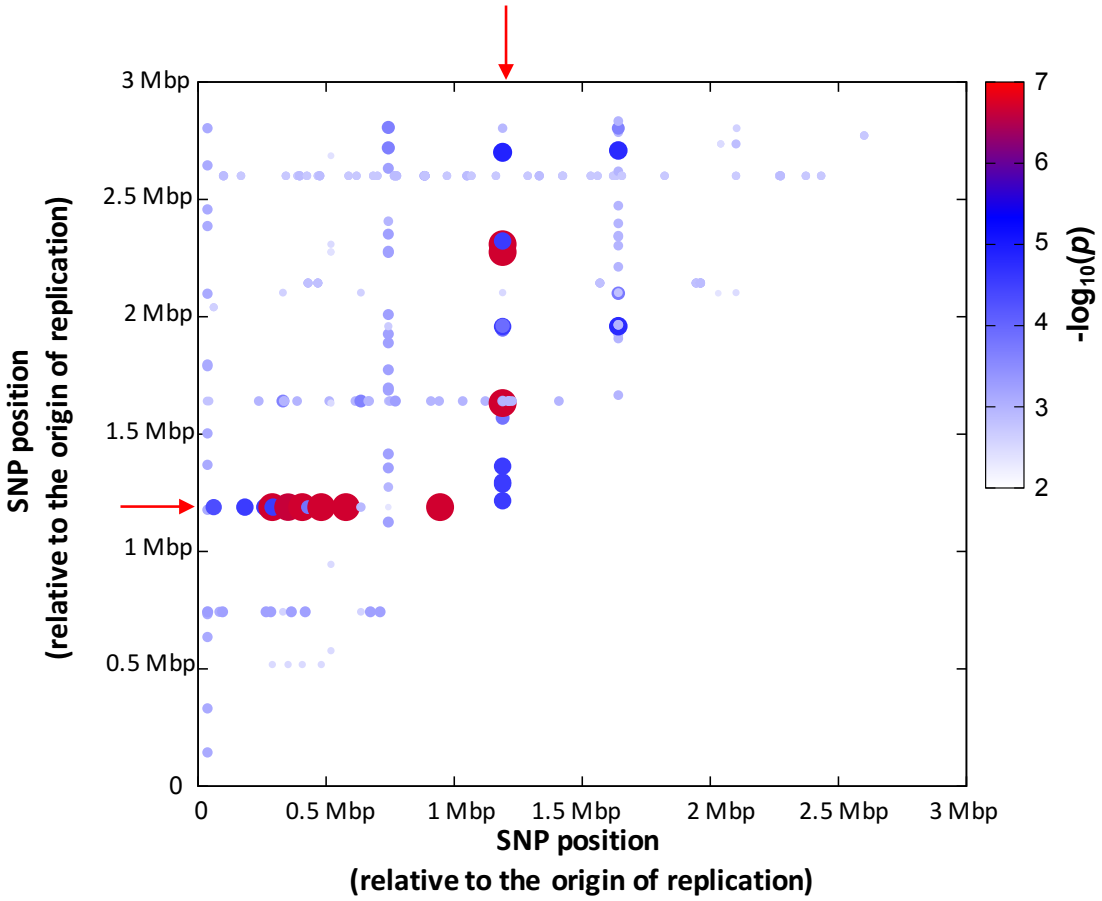

Fig. 1: Epistasis between the mupirocin resistance encoding mutation in the *ileS* gene and many other loci is associated with the toxicity of the USA300 lineage of MRSA. This heat map illustrates where specific combinations of the polymorphic site in the *ileS* gene and polymorphic sites elsewhere on the chromosome are associated with the toxicity of individual isolates. The mup^R conferring site is indicated on the X and Y axis by the red arrow.

bioRxiv preprint doi: https://doi.org/10.1101/148825; this version posted June 11, 2017. The copyright holder for this preprint (which was not certified by peer review) is the author/funder, who has granted bioRxiv a license to display the preprint in perpetuity. It is made available under aCC-BY-NC-ND 4.0 International license.

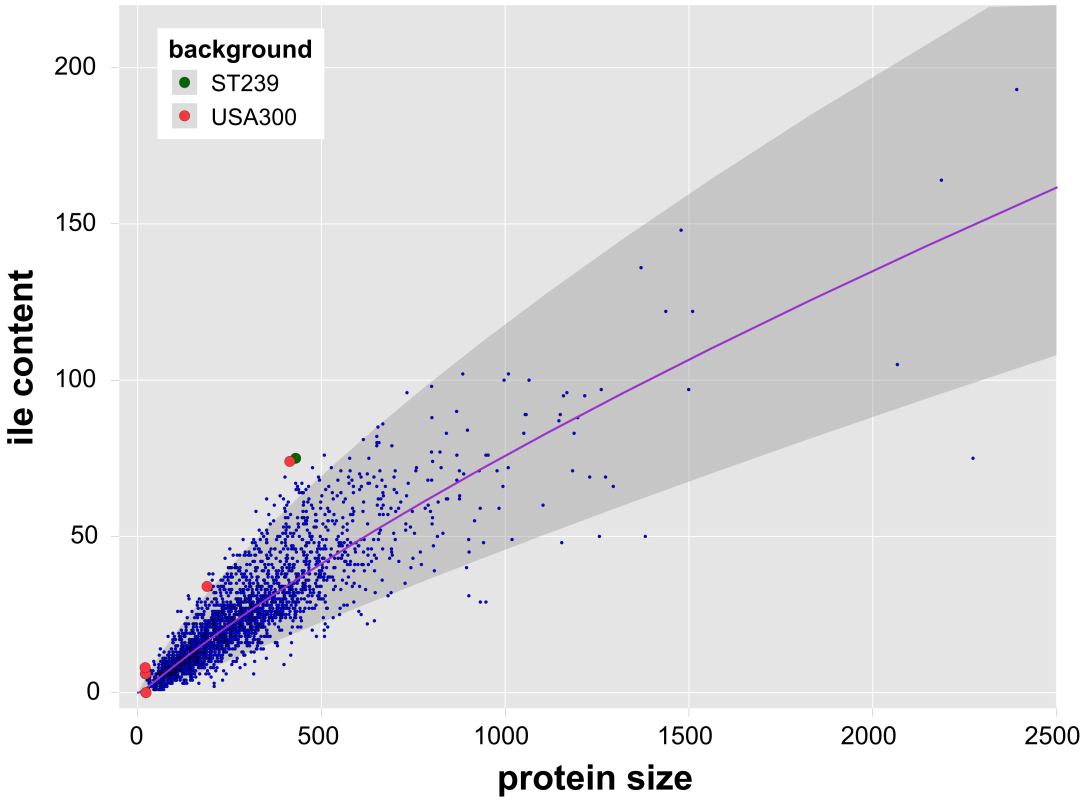

Fig. 2: The Ile content of *S. aureus* proteins relative to their length. The purple line shows the regression fit after transforming the data using the Box-Cox power transformation, with the shaded red area indicating the 95% prediction interval. The AgrC, AgrB and the PSMs with high ile content are indicated in green and red for the proteins encoded on the ST239 and USA300 background respectively.

bioRxiv preprint doi: https://doi.org/10.1101/148825; this version posted June 11, 2017. The copyright holder for this preprint (which was not certified by peer review) is the author/funder, who has granted bioRxiv a license to display the preprint in perpetuity. It is made available under aCC-BY-NC-ND 4.0 International license.

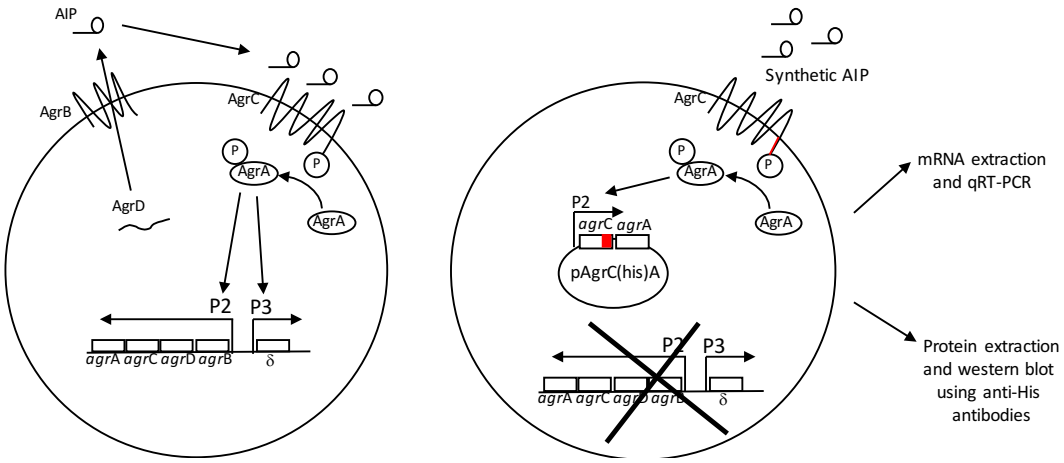

Fig. 3: Strain construction to facilitate the quantification of *agrC* transcription and translation. A: Depicts a native functioning Agr system. B: Depicts the mutant that was constructed and illustrates which elements of the Agr system were replaced to facilitate and control *agrC* transcription and translation. The his-tag fused to 3' end of *agrC* is depicted in red and is used to quantify AgrC protein using anti-his tag antibodies. The mupirocin sensitive version of this has been named MY42 and the mupirocin resistant version MY43.

bioRxiv preprint doi: https://doi.org/10.1101/148825; this version posted June 11, 2017. The copyright holder for this preprint (which was not certified by peer review) is the author/funder, who has granted bioRxiv a license to display the preprint in perpetuity. It is made available under aCC-BY-NC-ND 4.0 International license.

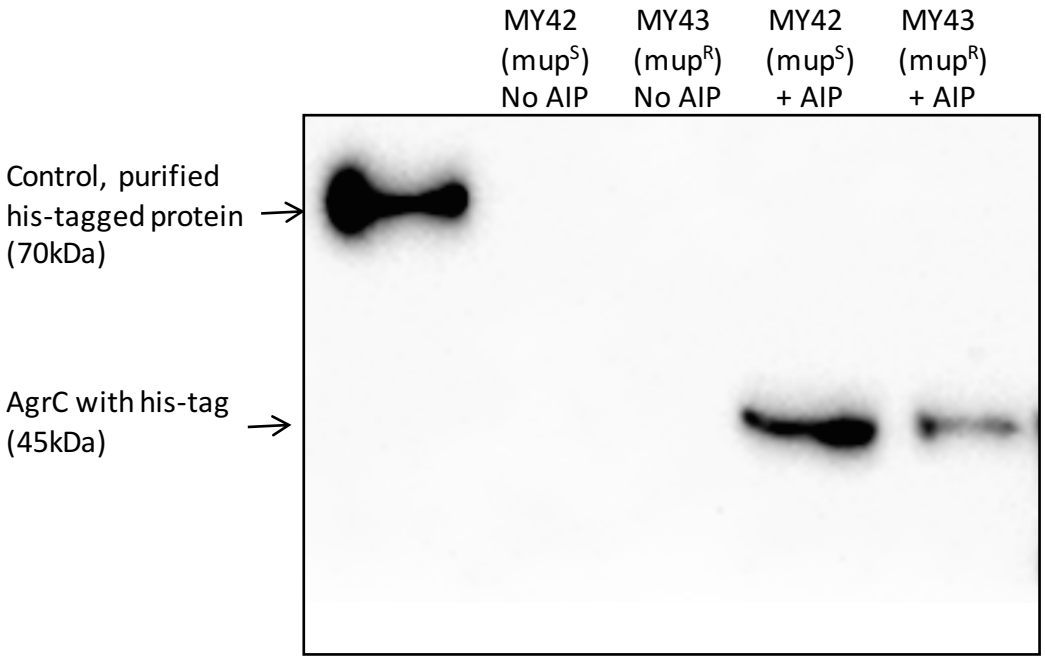

Fig. 4: Mupirocin resistance affects the translation of AgrC. Using the constructed strains MY42 and MY43 we compared the relative translation of AgrC using HisProbe HRP Conjugate (Thermo) to a 6X his-tag fused to the 5' end of the gene. The western blot demonstrates the effect of AIP induction of AgrC expression and the difference in translation of the AgrC protein when the strain is mupirocin resistant.

bioRxiv preprint doi: https://doi.org/10.1101/148825; this version posted June 11, 2017. The copyright holder for this preprint (which was not certified by peer review) is the author/funder, who has granted bioRxiv a license to display the preprint in perpetuity. It is made available under aCC-BY-NC-ND 4.0 International license.

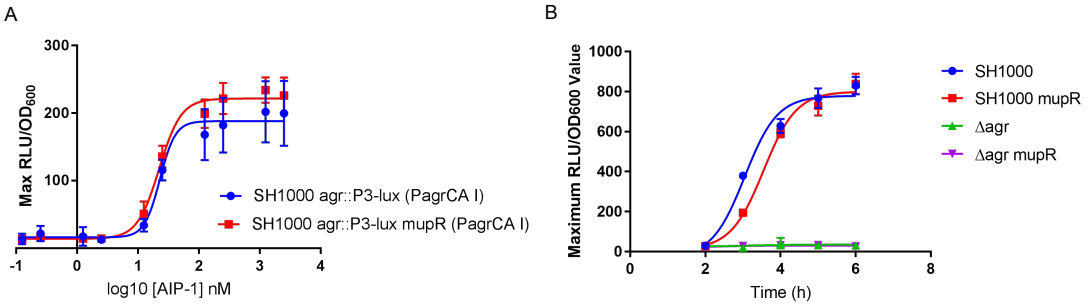

Fig. 5: Effect of mupirocin resistance on the response to exogenous AIP, and on AIP production as a function of growth. **A**: The half maximal effective concentration (EC_{50}) of AIP required to activate the Agr system was quantified for both the mupirocin resistant and sensitive *S. aureus* strains, where no significant effect of mupirocin resistance was observed. **B**: The relative concentration of AIP in the culture supernatant was quantified following growth for 6h for both the mupirocin resistant and sensitive strains. No effect of mupirocin resistance on this aspect of Agr activity was observed under these conditions.

bioRxiv preprint doi: https://doi.org/10.1101/148825; this version posted June 11, 2017. The copyright holder for this preprint (which was not certified by peer review) is the author/funder, who has granted bioRxiv a license to display the preprint in perpetuity. It is made available under aCC-BY-NC-ND 4.0 International license.

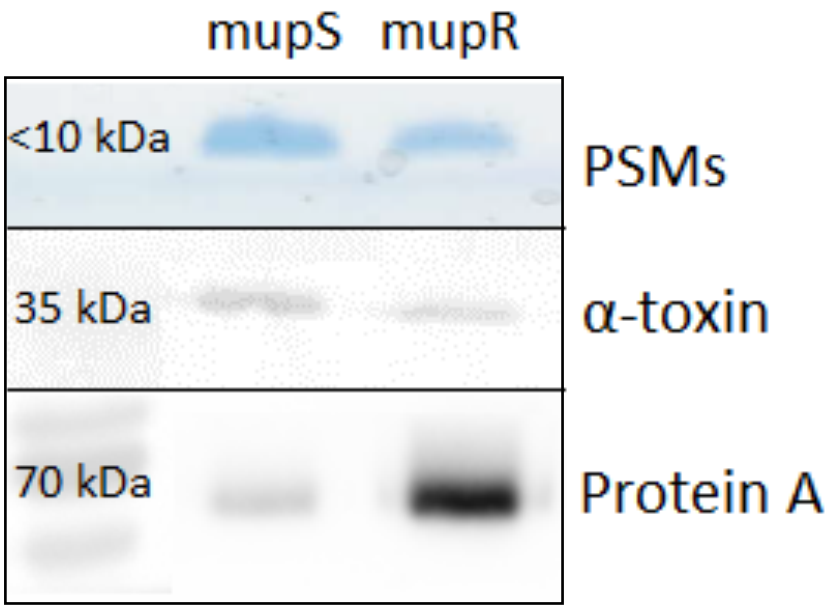

Fig. 6: Mupirocin resistance affects the expression of PSMS, alpha toxin and Protein A by *S. aureus* following growth in nutrient rich media. The mup^R and mup^S strains were grown in TSB for 18hrs. The PSMs were harvested by butanol extraction and run on an SDS-PAGE gel. Alpha toxin and protein A were western blotting using appropriate antibodies.

bioRxiv preprint doi: https://doi.org/10.1101/148825; this version posted June 11, 2017. The copyright holder for this preprint (which was not certified by peer review) is the author/funder, who has granted bioRxiv a license to display the preprint in perpetuity. It is made available under aCC-BY-NC-ND 4.0 International license.

TABLES

Table 1: Loci in both the ST239 and USA300 collections identified by GWAS as interacting epistatically with the mutation in *ileS.*

ST239

SNP position	Locus Tag/Gene Name	Putative function
1360889	SAWT20_12700	Putative DNA translocase (FtsK/SpoIIIE family protein)
1474673	SATW20_13760	Haloacid dehalogenase-like hydrolase superfamily protein
1536348	*ebh*	Very large surface anchored protein
1557020	*ebh*	Very large surface anchored protein
1557275	*ebh*	Very large surface anchored protein
1579791	*pbp2*	Penicillin-binding protein 2
1937314	SATW20_17780	Putative exported protein
1941832	SATW20_17820	Conserved hypothetical protein
1975607	SATW20_18180	Lantibiotic biosynthesis protein
2033565	SATW20_18600	ABC transporter ATP-binding protein
2075672	*pcrB*	pcrB family protein
2128192	SATW20_19530	β converting phage protein
2312226	SATW20_21880	ABC transporter ATP-binding protein
2409540	SATW20_22770	putative non-haem iron-containing ferritin
2432219	*fmtB*	LPXTG surface-anchored protein
2450342	Intergenic between SATW20_r160 AND SATW20_23010	16S rRNA AND conserved hypothetical protein
2548323	*modC*	Putative molybdenum transport ATP-binding protein
2578126	SATW20_24400	Putative bifunctional protein
2639747	*lldP2*	Putative L-lactate permease 2
2657438	Intergenic between SATW20_25130 AND *gltT*	Putative exported protein AND putative proton/sodium-glutamate symport protein
2674904	*nasD*	Nitrite reductase large subunit
2759775	SATW20_26050	Putative short chain dehydrogenase
2790429	SATW20_26280	Conserved hypothetical protein
2810368	Intergenic between SATW20_26460 AND SATW20_26470	Putative haloacid dehalogenase-like hydrolase AND ABC transporter ATP-binding protein
2970902	SATW20_27860	Hypothetical protein
3002241	*hisH*	Putative amidotransferase
3002845	*hisB*	Putative imidazoleglycerol-

bioRxiv preprint doi: https://doi.org/10.1101/148825; this version posted June 11, 2017. The copyright holder for this preprint (which was not certified by peer review) is the author/funder, who has granted bioRxiv a license to display the preprint in perpetuity. It is made available under aCC-BY-NC-ND 4.0 International license.

		phosphatedehydratase

1 **USA300**

SNP position	**Locus Tag/Gene Name**	**Putative function**
61025	SAUSA300_0050	Hypothetical protein
182746	*cap5I*	Capsular polysaccharide biosynthesis protein
260357	Intergenic between SAUSA300_0219 AND *pflB*	Putative iron compound A C transporter, iron compound-binding protein AND formate acetyltransferase
270510	SAUSA300_0226	3-hydroxyacyl-CoA dehydrogenase
289635	SAUSA300_0239	PTS system, fructose-specific enzyme II, BC component
292738	*gutB*	Sorbitol dehydrogenase
331125	SAUSA300_0279	Putative membrane protein
351171	SAUSA300_0300	Conserved hypothetical protein
406847	SAUSA300_0355	Acetyl-CoA acetyltransferase
429073	*ahpF*	Alkyl hydroperoxide reductase, subunit F
467549	SAUSA300_0414	Staphylococcal tandem lipoprotein
480640	SAUSA300_0426	Conserved hypothetical protein
577067	*cysE*	Serine acetyltransferase
635299	*vraB*	Acetyl-CoA c-acetyltransferase
742782	Intergenic between SAUSA300_0669 AND SAUSA300_0670	Undecaprenol kinase AND ABC transporter, ATP-binding protein, MsbA family
944770	Intergenic between *argG* AND *pgi*	Argininosuccinate synthase AND glucose-6-phosphate isomerase
1215913	*sun*	Ribosomal RNA small subunit methyltransferase B
1286986	*ftsK*	DNA translocase FtsK
1295497	*cinA*	Competence/damage-inducible protein cinA
1363207	*sbcC*	Exonuclease SbcC
1568945	SAUSA300_1403	phiSLT ORF412-like protein, portal protein
1632033	Intergenic between SAUSA300_1477 AND SAUSA300_1478	Transposase AND lipoprotein
1640549	SAUSA300_1485	Conserved hypothetical protein
1944161	Intergenic between *splA* AND SAUSA300_1759	Serine protease AND hypothetical protein
1961241	SAUSA300_1778	tRNA-asp
2102731	SAUSA300_1934	phi77 ORF020-like protein, phage major tail protein

bioRxiv preprint doi: https://doi.org/10.1101/148825; this version posted June 11, 2017. The copyright holder for this preprint (which was not certified by peer review) is the author/funder, who has granted bioRxiv a license to display the preprint in perpetuity. It is made available under aCC-BY-NC-ND 4.0 International license.

2275521	SAUSA300_2106	Putative transcriptional repressor
2276564	*mtlA*	PTS system, mannitol specific IIA component
2308707	SAUSA300_2135	Iron compound ABC transporter, permease protein
2322700	SAUSA300_2146	Alcohol dehydrogenase, zinc-containing
2685939	SAUSA300_2486	Putative ATP-dependent Clp proteinase
2700617	SAUSA300_2497	Aminotransferase, class I
2803422	SAUSA300_2583	Putative glycosyl transferase

Table 2: The effect of mupirocin resistance on the relative transcription and translation of AgrC. Transcription was measured by qRT-PCR and is presented relative to *gyrB* transcription. Translation was measured by western blotting using anti-hiss tag antibodies and densitometry used to quantify the amount of protein present. This was performed in triplicate and a representative western is present in figure 3.

	MY42 (mup^S)	**MY43 (mup^R)**	**Ratio**	**P value**
Transcription	**0.95**	**0.98**	**0.97**	**0.17**
Translation	**4771**	**2305**	**2.07**	**0.006**

Table 3: Strains used in this study.

Strain	**Relevant genotypic information**	**Mupirocin resistance**
SH1000	wild-type lab strain	mup^S
MY40	mupirocin resistant SH1000	mup^R
MY18	SH1000 Δagr	mup^S
MY41	mupirocin resistant MY18	mup^R
MY42	MY18 + pAgrC(his)A	mup^S
MY43	MY41 + pAgrC(his)A	mup^R